# Auto-adaptive velocity feedback for active isolation of random vibrations in subcritical 2 dof systems

**N. Alujevic[1], H. Wolf[2], Z. Domazet[1]**
[1] University of Split, FESB
R. Boskovica 21, 21000, Split, Croatia
e-mail: **neven.alujevic@fesb.hr**

[2] University of Zagreb, FSB
I. Lucica 5,10000, Zagreb, Croatia

## Abstract
Skyhook damping is an active vibration isolation method, which can also be used to reduce vibration transmission between masses in lumped parameter 2 degree of freedom (dof) systems. The method is based on measuring the absolute velocity of the clean body, multiplying it by a negative gain, and feeding the result back to a force actuator reacting between the clean and the dirty body. In such a way disturbances coming onto the clean body from the dirty body can be successfully rejected in a broad frequency band. However, the method is only suitable if the feedback loop is unconditionally stable such that appropriately high feedback gains can be applied. It has been previously shown that passive 2 dof systems can be classified as so called sub- or supercritical based on whether the skyhook damping loop is conditionally or unconditionally stable. For subcritical systems the absolute velocity feedback loop is conditionally stable and a skyhook damping approach is consequently not appropriate due to a control spillover effect at the first resonance frequency. In such a case the feedback loop can be stabilized by including an appropriate amount of relative damping between the clean and the dirty body in addition to the skyhook damping. This approach has been referred to as blended velocity feedback. In this paper the application of the blended velocity feedback on a subcritical 2dof system is investigated using an auto-tuning controller. An algorithm to gradually change the relative and absolute feedback gains until the active isolation performance reaches its best by applying an optimal combination of the two gains is applied. It is shown that there is only one such optimal combination, that is, the performance surface has a global minimum. Furthermore there are no local minima so a trial and error algorithm can be applied. Although in the frequency domain finding the minimum of the performance surface is straightforward, in the time domain the determining the clean body mean squared velocity can take a considerable time per step of the algorithm, such that the convergence of the trial and error algorithm can be relatively slow. It is hypothesized that a model based approach in determining the step size may speed-up the convergence.

## 1 Introduction

Skyhook damping is an active approach to vibration isolation where a force actuator is used in parallel with the passive isolator (e.g. a spring and a dashpot) between two structures: the dirty structure and the clean structure [1,2]. The aim of the active isolation is to reduce vibrations of the clean structure. The actuator between the two structures is driven with a signal proportional to the negative absolute velocity of the clean structure. With such approach the ratio of vibration amplitudes between the clean and the dirty structure gets reduced at low frequencies and rolls-off steeply at high frequencies [1-3]. On the contrary, with classical passive isolators this is usually not possible because the high frequency roll-off is traded for low frequency resonance attenuation [1,4,5]. Therefore, skyhook damping approach is an attractive

vibration isolation option in cases where excitation is broadband such that good isolation performance at both low and high frequencies is required.

However, not any pair of structures is a suitable for the application of skyhook damping active isolators. A number of studies have indicated cases where the skyhook damping control loop tends to be destabilized by the dynamical response of the two structures [6-8]. A recent study performed on lumped parameter two degree of freedom (dof) systems has also dealt with this problem [9]. The authors considered the use of skyhook damping with the aim to protect 1 dof subsystem from vibrations coming through a connecting spring from another 1 dof subsystem. The whole arrangement can therefore be viewed as a 2 dof system where the perimeter springs are both connected to fixed bases and the two masses are coupled in the middle via the connecting spring. The principal results of the study [9] can be summarized as follows. If the resonance frequency of the dirty 1 dof system is lower than the resonance frequency of the clean 1 dof system, the skyhook damping loop can be conditionally stable even with ideal velocity sensor and force actuator. The feedback control gain margin is in fact a matter of how much residual passive damping exists in the system. If the resonance frequency of the dirty 1 dof system is higher than the resonance frequency of the clean 1 dof system, the skyhook damping loop is always unconditionally stable if ideal sensor and actuators are used. The former family of 2dof systems is called subcritical and the latter family is called supercritical systems [9].

Subcritical isolation problems can be treated by implementing an amount of relative damping between the two masses, either active or passive, in addition to the active skyhook damping. In fact, it is possible to design unconditionally stable feedback loops if two absolute velocities of the dirty and the clean mass are linearly combined into the error signal using a ratio of the two velocity feedback gains larger than a critical one. (Using such a linear combination is fully equivalent to providing simultaneously relative and absolute active damping.) The critical ratio can be calculated as a function of the two masses and the three spring stiffnesses, as shown in [9]. Such “blended” velocity feedback can be used not only for stabilizing the loop but also for efficient active vibration isolation in a large group of subcritical 2dof systems. However, it is necessary that the correct blending coefficient (the ratio of the two absolute velocities taken from the two masses) and the correct feedback gain are used [9].

This study is focused onto how to set the correct blending coefficient and the correct feedback gain, in an automated online process. This is done using a trial and error algorithm which monitors the clean body mean squared vibration velocity and changes the two control parameters in order to minimize the clean body vibration in a number of discrete steps. The study is performed theoretically, using a state space model of the active vibration isolation in a subcritical 2dof system. The time-domain simulation results are also checked against the frequency domain results. In order to make sure that the time domain model is fully equivalent to the frequency domain model, and that the results are comparable, the state space formulation is directly derived from the previously developed frequency domain model.

The paper is structured into five sections. In the second section the model problem is given including the definition of the sub- and supercritical systems, as well as defining the metrics used for the vibration isolation performance assessment. In the third section the state-space model is developed from the frequency domain model. In addition, it is explained how the time varying systems due to the sequential adaptation of the control parameters can be treated through simulating a sequence of successive time invariant systems. In the fourth section the auto-tuning process is simulated and the simulation results are discussed.

# 2 The description of model problem

## 2.1 Subcritical and supercritical 2dof systems

As shown in Figure 1 the system studied consists of two masses $m_1$ and $m_2$ coupled by the spring between them $k_2$ and also attached to the fixed reference base via the two mounting springs $k_1$ and $k_3$. It

is assumed that the damping in the system is light and can be represented for both modes through one modal damping ratio $\eta_1 = \eta_2 = \eta$ .

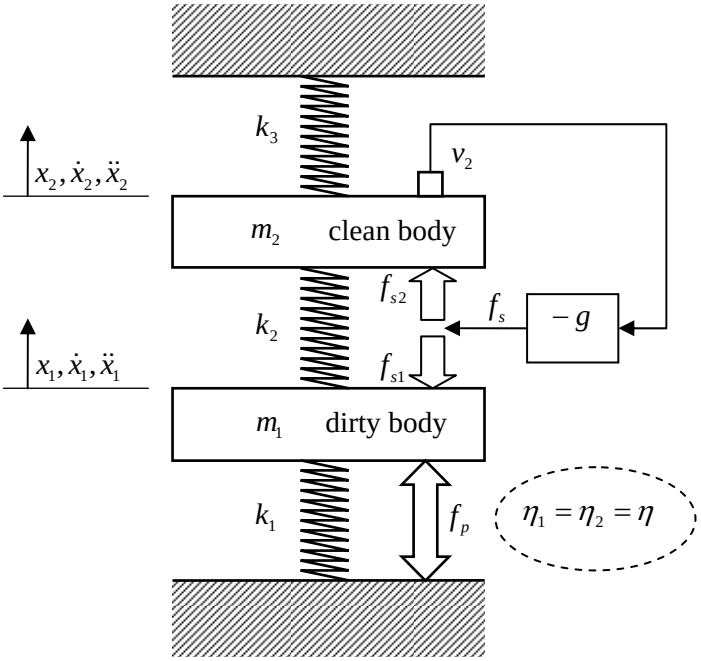


Figure 1: Skyhook active damping in a 2dof mechanical system

The lower mass $m_1$ is excited by the broadband primary force $f_p$ . In this study it is assumed that nothing is a priori known about the excitation, such that the primary force is anticipated that has a white noise spectral distribution. The vibration isolation objective in this study is to minimise vibrations of the upper mass $m_2$ relative to the primary excitation force $f_p$ , that is, the goal of the active control is to minimise the amplitude of the transmissibility function, $\left|v_2 / f_p\right|$ , over the whole range of frequencies laying between 0 and $\infty$ Hz. The secondary control force $f_s$ is implemented through a reactive actuator between the two masses which, as shown in the figure, is driven by the absolute velocity of the clean body, $v_2$ , which in fact is an application of a skyhook damper. It has been shown in [9] that such a feedback loop is always unconditionally stable (assuming ideal transducers) if:

$$\frac{k_1}{m_1} > \frac{k_3}{m_2} . \tag{1}$$

Equation (1) indicates that the resonance frequency, $\Omega_1 = \sqrt{k_1 / m_1}$ , of the lower mass suspended only through the lower mounting spring $k_1$ only has to be larger than the resonance frequency $\Omega_2 = \sqrt{k_3 / m_2}$ of the upper mass suspended only through the upper mounting spring $k_3$ in order for the feedback loop to be unconditionally stable. In other words there are two families of all passive systems shown in Figure 1, regarding the stability of the skyhook damper: supercritical systems that satisfy inequality (1), and subcritical systems which do not satisfy inequality (1). With supercritical system the skyhook damping approach yields unconditionally stable feedback loops. The skyhook damping applied on subcritical 2 dof systems yields conditionally stable feedback loops, unless the passive damping ratio is rather large and the two resonances of the system are not well separated [9]. With subcritical systems the vibration isolation objective cannot be accomplished in a broad frequency band using only the upper mass absolute velocity feedback. This is because of the clean body response magnification at the first resonance frequency which

cancels the reduction at the second resonance frequency [9]. However, for performing the active vibration isolation on subcritical systems a blended velocity feedback may be used and its application is described in the following subsection.

## 2.2 Blended velocity feedback

The implementation of the blended velocity feedback loop is based on producing both relative and sky-hook damping effects. The error velocity is formed as a blended combination of the upper mass velocity $v_2$ and the lower mass velocity $v_1$ according to the following expression:

$$v_e = v_2(1-\alpha) - v_1\alpha \,. \tag{2}$$

Schematically, this approach is shown in Figure 2.

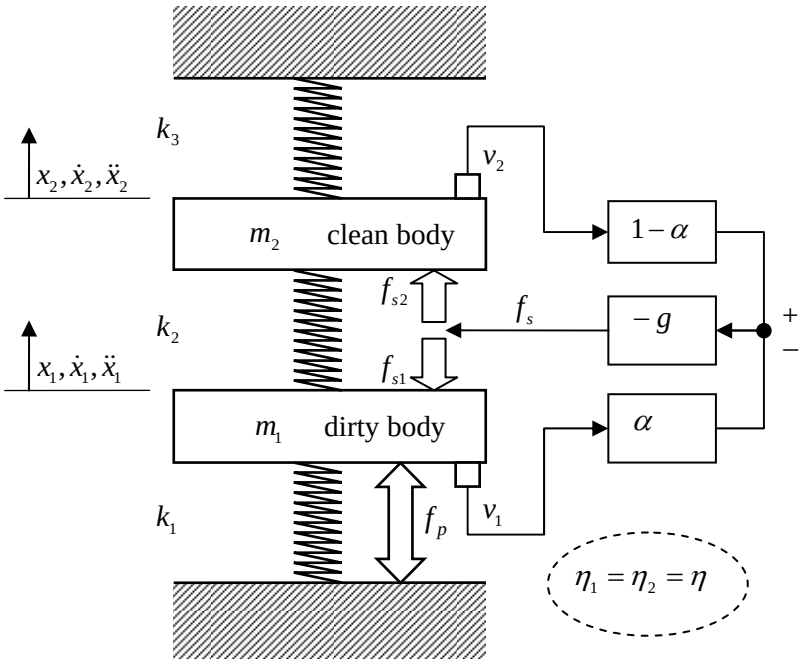


Figure 2: Blended velocity feedback in a 2dof mechanical system

This formulation of the error signal allows for varying the velocity weighting coefficient $\alpha$ between 0 and 1. Therefore, it is possible to apply various types of the velocity feedback control as indicated in Table 1.

| | |
|---|---|
| $\alpha = 0$ | $v_e = v_2$, upper mass absolute velocity feedback (sky-hook damping) |
| $\alpha \in \langle 0,0.5 \rangle$ | Upper mass velocity + relative velocity feedback |
| $\alpha = 0.5$ | $v_e = v_2 - v_1$, relative velocity feedback (passive damping) |
| $\alpha \in \langle 0.5,1 \rangle$ | Lower mass velocity + relative velocity feedback |
| $\alpha = 1$ | $v_e = -v_1$, lower mass absolute velocity feedback |

Table 1: The error signals as a result of the use of different velocity weighting coefficients $\alpha$.

Note that the blended velocity feedback could be applied in practice by using a passive damper with tuneable damping coefficient and a reactive actuator between the two masses in conjunction with a

velocity sensor on the upper mass ($\alpha \in \langle 0,0.5 \rangle$) or on the lower mass ($\alpha \in \langle 0.5,1 \rangle$)which implement a velocity feedback loop through an appropriate feedback gain. Thus in practice only one sensor would be used. However, for simplicity reasons, the mathematical model of passive and active systems studied which is formulated next is performed by assuming the use of two sensors and it is implicitly understood that in practice one of the two velocity sensors would not be necessary.

The frequency averaged transmissibility, given by

$$T = \int_{-\infty}^{\infty} \left| \frac{v_2}{f_p}(\omega) \right|^2 d\omega , \tag{3}$$

is used as the metrics for the quality of the vibration isolation performance throughout this paper. As it is further discussed in Section 4 of the paper, the frequency averaged transmissibility, *T*, can be minimized if the correct pair of the blending coefficient $\alpha$ and the feedback gain $g$ is used. Thus, it might be possible, assuming that the primary force has a constant time-averaged spectral distribution, to monitor how the time-averaged squared velocity of the clean body, $v_2$ , changes with small variations in the feedback gain *g* and the blending coefficient $\alpha$, in order to drive the metrics given in Equation (3) to a minimum. This would in fact represent an adaptive controller which tunes itself to the optimum pair of control parameters.

# 3 The mathematical model

## 3.1 Frequency domain formulation

The transmissibility function, $v_2 / f_p$ , which is in fact the transfer mobility between the clean body and the dirty body with the active control loop engaged can be expressed as a function of frequency through a ratio of polynomials with the maximum order of four [9]:

$$\frac{v_2}{f_p}(\omega) = \frac{B_0 + i\omega B_1 - \omega^2 B_2 - i\omega^3 B_3}{A_0 + i\omega A_1 - \omega^2 A_2 - i\omega^3 A_3 + \omega^4 A_4} . \tag{4}$$

where $i = \sqrt{-1}$, and coefficients $A_0 ... A_4$ and $B_0 \ldots B_3$ have been calculated as functions of the parameters of the system under control ($m_1, m_2, k_1, k_2, k_3, \eta, g$, and $\alpha$) and can be found in Reference [9]. The solution to the integral given in Equation (3) for functions of a polynomial type as that given in Equation (4) can be expressed as [10]:

$$T = \pi \frac{A_0 B_3^2 (A_0 A_3 - A_1 A_2) + A_0 A_1 A_4 (2B_1 B_3 - B_2^2) - A_0 A_3 A_4 (B_1^2 - 2B_0 B_2) + A_4 B_0^2 (A_1 A_4 - A_2 A_3)}{A_0 A_4 (A_0 A_3^2 + A_1^2 A_4 - A_1 A_2 A_3)} . \tag{5}$$

On the other hand, the point mobility of the dirty body $v_1 / f_p$ with active control is necessary in order to fully describe the system, too. This is also a function of frequency through a ratio of polynomials with the maximum order of four. The denominator is the same as that in Equation (4) but the numerator is different:

$$\frac{v_1}{f_p}(\omega) = \frac{C_0 + i\omega C_1 - \omega^2 C_2 - i\omega^3 C_3}{A_0 + i\omega A_1 - \omega^2 A_2 - i\omega^3 A_3 + \omega^4 A_4} \tag{6}$$

The coefficients $C_0 \ldots C_3$ are given below:

$$C_0 = 0 , \tag{7}$$

$$C_1 = -S^2 (V + U)(P - Q^2) , \tag{8}$$

$$C_2 = S^2(P-Q^2)\left[4Pg(\alpha-1)-\eta\left(\frac{V}{\sqrt{\frac{Q-\sqrt{P}}{R}}}+\frac{U}{\sqrt{\frac{Q+\sqrt{P}}{R}}}\right)\right], \tag{9}$$

$$C_3 = RS^2\left|(V-U)\sqrt{P}+(V+U)Q\right|. \tag{10}$$

The substitution coefficients P, Q, R, S, T, U and V depend only on the 2 dof system passive parameters ($m_1$, $m_2$, $k_1$, $k_2$, and $k_3$) and can be found in [9].

## 3.2 State space formulation

The standard state space formulation matrices **A**, **B**, **C**, and **D** for the controller canonical form of the system at hand, are populated as follows:

$$\mathbf{A} = \begin{bmatrix} 0 & 0 & 1 & 0 \\ 0 & 0 & 0 & 1 \\ a_{31} & a_{32} & a_{33} & a_{34} \\ a_{41} & a_{42} & a_{43} & a_{44} \end{bmatrix}, \tag{11}$$

$$\mathbf{B} = \begin{Bmatrix} 0 & 0 & b_{31} & 0 \end{Bmatrix}^T, \tag{12}$$

$$\mathbf{C} = \begin{bmatrix} 1 & 0 & 0 & 0 \\ 0 & 1 & 0 & 0 \end{bmatrix}, \tag{13}$$

$$\mathbf{D} = \begin{Bmatrix} 0 & 0 \end{Bmatrix}^T, \tag{14}$$

assuming that the input into the system is a point force acting on the dirty body and the states of the system are the two displacements and the two velocities:

$$\mathbf{X} = \begin{Bmatrix} x_1 & x_2 & \dot{x}_1 & \dot{x}_2 \end{Bmatrix}^T, \tag{15}$$

such that:

$$\dot{\mathbf{X}} = \mathbf{A}\mathbf{X} + \mathbf{B}u, \tag{16a}$$

$$\mathbf{Y} = \mathbf{C}\mathbf{X} + \mathbf{D}u, \tag{16b}$$

where $u$ is the input to the system which for the system studied is the primary force $f_p(t)$. Taking the Laplace transformation of both sides of Eq (16) gives:

$$s\mathbf{X}(s) = \mathbf{A}\mathbf{X}(s) + \mathbf{B}u(s), \tag{17a}$$

$$\mathbf{Y}(s) = \mathbf{C}\mathbf{X}(s) + \mathbf{D}u(s), \tag{17b}$$

such that, after the elimination of $\mathbf{X}(s)$ from Equations (17a,b) and some mathematical manipulations, the transfer function representation of the system is given by:

$$\mathbf{Y}(s)/u(s) = \mathbf{G}(s) = \left\{\mathbf{C}(s\mathbf{I}-\mathbf{A})^{-1}\mathbf{B}+\mathbf{D}\right\}, \tag{18}$$

where $s = i\omega$, and **I** is the identity matrix. **G** is a 2×1 vector containing the point receptance of the dirty body in the first row, and the transfer receptance of the system in the second row in the polynomial form. Substituting Equations (11-14) into (18) yields these polynomial coefficients represented through the elements $a_{i,j}$ and $b_{i,j}$ given in (11-14):

$$\mathbf{G}(s)=\left\{\begin{array}{c}\dfrac{-(-s^2+a_{44}s+a_{42})b_{31}}{a_{42}a_{31}-a_{41}a_{32}+s(a_{44}a_{31}-a_{43}a_{32}+a_{42}a_{33}-a_{41}a_{34})+s^2(-a_{43}a_{34}-a_{31}+a_{44}a_{33}-a_{42})-s^3(a_{33}+a_{44})+s^4}\\ \dfrac{(a_{43}s+a_{41})b_{31}}{a_{42}a_{31}-a_{41}a_{32}+s(a_{44}a_{31}-a_{43}a_{32}+a_{42}a_{33}-a_{41}a_{34})+s^2(-a_{43}a_{34}-a_{31}+a_{44}a_{33}-a_{42})-s^3(a_{33}+a_{44})+s^4}\end{array}\right\} \quad (19)$$

The system mobilities are obtained by multiplying receptances in Eq. (19) by *s*:

$$\frac{v_1}{f_\mathrm{p}}=\frac{b_{31}s^3+b_{31}a_{44}s^2+b_{31}a_{42}s}{a_{42}a_{31}-a_{41}a_{32}+s(a_{44}a_{31}-a_{43}a_{32}+a_{42}a_{33}-a_{41}a_{34})+s^2(-a_{43}a_{34}-a_{31}+a_{44}a_{33}-a_{42})-s^3(a_{33}+a_{44})+s^4} \quad (20a)$$

$$\frac{v_2}{f_\mathrm{p}}=\frac{b_{31}a_{43}s^2+b_{31}a_{41}b_{31}}{a_{42}a_{31}-a_{41}a_{32}+s(a_{44}a_{31}-a_{43}a_{32}+a_{42}a_{33}-a_{41}a_{34})+s^2(-a_{43}a_{34}-a_{31}+a_{44}a_{33}-a_{42})-s^3(a_{33}+a_{44})+s^4} \quad (20b)$$

Equations (4 and 6) can be normalised such that the term multiplying $\omega^4$ becomes unity, that is the numerator and the denominator can be divided by $A_4$. Then, by equating the new, normalised coefficients, $A_0'=A_0/A_4, A_1'=A_1/A_4 \ldots A_4'=1, B_0'=B_0/A_4, B_1'=B_1/A_4 \ldots B_3'=B_3/A_4$, $C_0'=C_0/A_4, C_1'=C_1/A_4 \ldots C_3'=C_3/A_4$ to the terms multiplying the corresponding powers of *s* in Eqs. (20a,b), the elements of the **A** and **B** matrices are calculated as follows:

$$a_{31}=\frac{(-A_2'C_3'^2+(A_3'C_2'+C_1')C_3'-C_2'^2)B_1'^2+B_2'(-C_1'C_3'A_3'+A_1'C_3'^2+C_2'C_1')B_1'-A_0'C_3'^2B_2'^2}{C_3'\left(-B_1'C_2'B_2'+B_1'^2C_3+C_1'B_2'^2\right)},$$

$$a_{32}=\frac{-B_1A_0C_3^3+((-B_2A_1+B_1A_2)C_1+C_2A_0B_2)C_3^2-C_1((B_1-A_3B_2)C_1+C_2B_1A_3)C_3+C_1C_2(-B_2C_1+B_1C_2)}{C_3'\left(-B_1'C_2'B_2'+B_1'^2C_3+C_1'B_2'^2\right)},$$

$$a_{33}=C_2'/C_3'-A_3',$$

$$a_{34}=\frac{\begin{array}{c}(A_0'B_2'-B_1'A_1')C_3'^3+\left[(C_2'A_2'+C_1'A_3')B_1'-C_1'B_2'A_2'\right]C_3'^2+\\ +\left[(-2C_2'C_1'-C_2'^2A_3')B_1'+B_2'C_1'(A_3'C_2'+C_1')\right]C_3'+B_1'C_2'^3-C_1'B_2'C_2'^2\end{array}}{C_3'\left(-B_1'C_2'B_2'+B_1'^2C_3+C_1'B_2'^2\right)}, \quad (21a\text{-}i)$$

$$a_{41}=B_1'/C_3',$$

$$a_{42}=C_1'/C_3',$$

$$a_{43}=B_2'/C_3',$$

$$a_{44}=-C_2'/C_3',$$

$$b_{31}=C_3'.$$

The state space model allows for a simulation of the system response to an arbitrary input, i.e. to the excitation by a random primary force with flat spectral distribution, if the system is time-invariant. However, as the purpose of the study is to investigate the tuning of the control parameters *g* and $\alpha$, the system in fact changes with time. Each time a gain and/or the blending coefficient change, the coefficients in Eq. (21) also change. On the other hand, between two adjacent corrections of the control parameters the system is time invariant. It is thus possible to use this fact and to simulate the tuning process via a sequence of simulations of different systems which are at the time of control parameter change linked by positions and velocities of the two masses. In other words, at the time of adjusting control parameters, the instantaneous states of the systems are recorded and used as initial conditions for a new linear time invariant system. This is how the simulations in the following subsections were performed. For the purpose of numerical efficiency, it is needed to have the algebraic expressions for the system parameters as given in Eq. (21).

# 4 Auto-adaptive blended velocity feedback

In this subsection the auto-adaptive blended velocity feedback is studied on an example system. As previously mentioned, the metrics for the performance of the active isolation is the frequency averaged modulus of the transfer mobility of the system, given in Equation (3). In the remaining of this paper this quantity is normalized with reference to the "open-loop" case, that is, it is normalised to the frequency averaged modulus of the transfer mobility of the passive system. Therefore the forthcoming simulation results are discussed in terms of the Frequency Averaged Reduction (FAR) which is therefore solely due to the active control:

$$FAR = \frac{T_{CONTROL}}{T_{NO\_CONTROL}} = \frac{\left[\int_{-\infty}^{\infty}\left|\frac{v_2}{f_p}(\omega)\right|^2 d\omega\right]_{\substack{g\neq 0\\ \alpha\neq 0}}}{\left[\int_{-\infty}^{\infty}\left|\frac{v_2}{f_p}(\omega)\right|^2 d\omega\right]_{g=0}} \tag{22}$$

An example system is studied which has the passive parameters listed in the first six columns of Table 2. It can be seen that the passive system is subcritical because the stiffness $k_1$ is zero and thus the inequality given in (1) is not satisfied.

| Property | $m_1$ (kg) | $m_2$ (kg) | $k_1$ (N/m) | $k_2$ (N/m) | $k_3$ (N/m) | $\eta$ (-) | $\alpha_{opt}$ (-) | $g_{opt}$ (Ns/m) |
|---|---|---|---|---|---|---|---|---|
| Value | 1 | 0.3 | 0 | 20769 | 3000 | 0.01 | 0.84 | 302 |

Table 2: The example system properties

Figure 3 shows the FAR surface, calculated according to Eq. (22) as a function of the control parameters $g$ and $\alpha$. The use of the blending coefficients in the range shown on the $y$-axis results in unconditionally stable feedback loops. In other words, a feedback loop working with $\alpha < 0.47$ would have been conditionally stable, as 0.47 is the critical blending coefficient for the passive system at hand. (See Reference [9].)

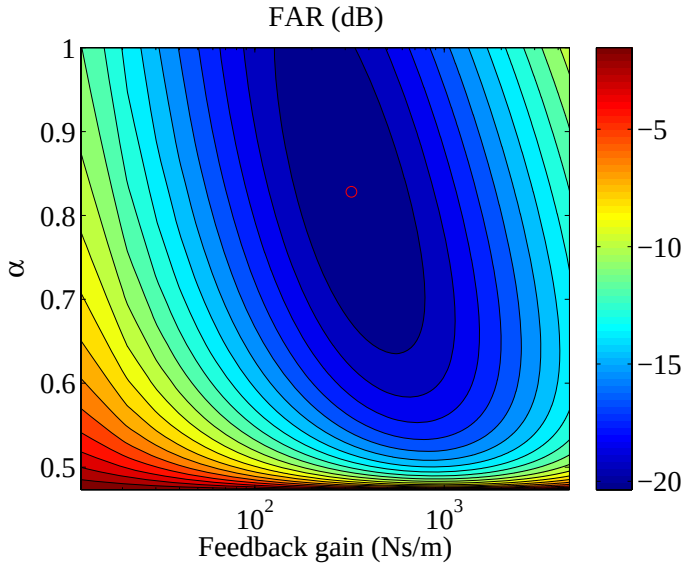


Figure 3: The Frequency Averaged Reduction (FAR) as a function of the two control parameters

The figure reveals two important facts. First, the depicted surface has a global minimum which is obtained if an optimum combination of the control parameters is used. This minimum is indicated by the red circle. Second, this optimal combination cannot be achieved with passive control because the optimum blending coefficient is about 0.84. In other words skyhook damping is needed in addition to the relative damping in order to reach the optimum. Therefore it is clear that for the system studied the blended velocity feedback can outperform a passive isolator whose effects may be viewed as the blended velocity feedback with $\alpha = 0.5$ (see Table 1).

Based on the above observations, a controller with an adaptive control parameters g and $\alpha$ could be able to reach a set of optimum parameters by monitoring the time averaged mean squared velocity of the clean body as an algorithm goes down the performance surface depicted in Figure 3. This is because the time averaged mean squared velocity of the clean body should converge to a value if it is averaged over a sufficiently long time period. Hence a trial and error algorithm is studied here which successively changes the control parameters by small increments according to the following rules:

$$g(\mathrm{n}+1) = g(\mathrm{n}-1) + inc_{\mathrm{g}} \cdot \mathrm{sign}[\bar{v}_2^2(\mathrm{n}-1) - \bar{v}_2^2(\mathrm{n})], \text{ even step number n,} \tag{23}$$

$$\alpha(\mathrm{n}+1) = \alpha(\mathrm{n}-1) + inc_{\alpha} \cdot \mathrm{sign}[\bar{v}_2^2(\mathrm{n}-1) - \bar{v}_2^2(\mathrm{n})], \text{ odd step number n,} \tag{24}$$

where $\bar{v}_2^2(\mathrm{n}-1)$ is the "old" time averaged squared velocity of the clean body, and $\bar{v}_2^2(\mathrm{n})$ is the current time averaged squared velocity of the clean body. Thus, after an increase of the feedback gain by a small gain increment $inc_{\mathrm{g}}$, the algorithm checks if the "old" time averaged squared velocity is larger than the current one. If so, after two steps the feedback gain gets increased again. In between, the $\alpha$ is increased by an increment $inc_{\alpha}$. The algorithm again checks if the "old" time averaged squared velocity is larger than the current one. If so, after two steps the $\alpha$ gets increased again. This procedure is repeated until a further increase in a control parameter results in the current time averaged squared velocity being larger than that from the previous step. In such a case the corresponding control parameter gets decreased by its increment after two steps. Figure 4 shows the convergence behavior of such an algorithm applied onto the example system with properties as given in Table 2. The primary force excitation was such that the spectral distribution of the force is white noise with a time-averaged mean squared amplitude of one.

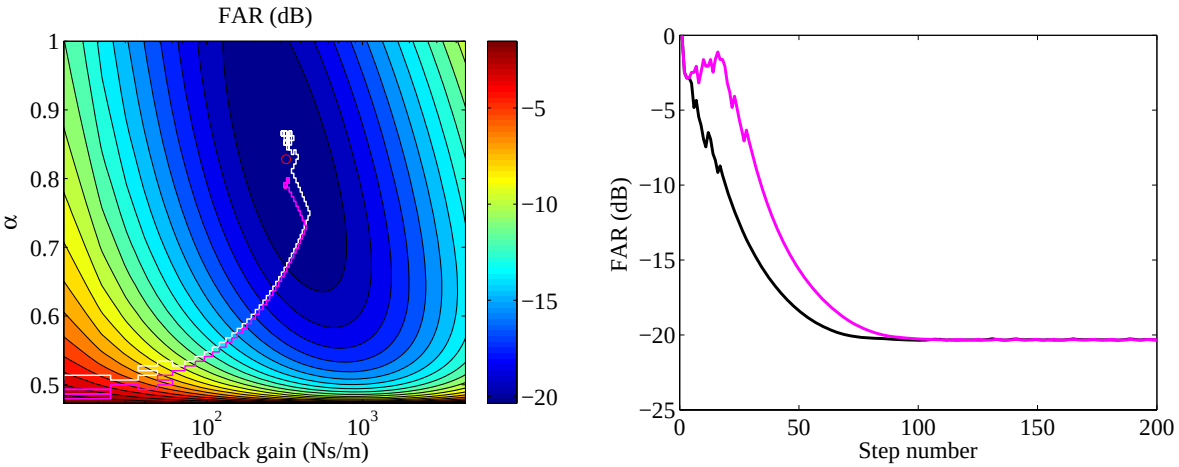


Figure 4: The convergence behaviour of the auto-adaptive controller

The algorithm was allowed to perform 200 steps with the increment in the feedback gain $inc_{\mathrm{g}} = g_{opt}/25$ and the increment in the blending coefficient $inc_{\alpha} = \alpha_{opt}/50$. The optimal blending coefficients and the feedback gain are listed in Table 2. The controller parameters at the start of the simulation were $g$=0, and $\alpha = 0.5$. The mean squared velocity of the clean body was estimated through averaging during a fixed period of 5 seconds per each step. As can be seen in Figure 4 two simulations were performed which result in different convergence trajectories shown by the black/white and magenta lines in the two plots. The

reason for different convergence trajectories is merely the fact that the primary force is random, and thus for the two simulations the primary force time histories were different. The right hand side plot in Figure 4 shows that the optimum set of control parameters is reached after about 100 steps for both cases. The left hand side plot in Figure 4 indicates that the optimum feedback gain is reached more quickly than the optimum $\alpha$. This can be explained through the fact that the increment for the blending coefficient is smaller relative to its optimum value when compared to the increment for the feedback gain relative to its optimum value. As shown in Figure 5 the total time until the algorithm converges is about 500 seconds (or about 8 minutes) in both cases which can be seen as a relatively slow convergence.

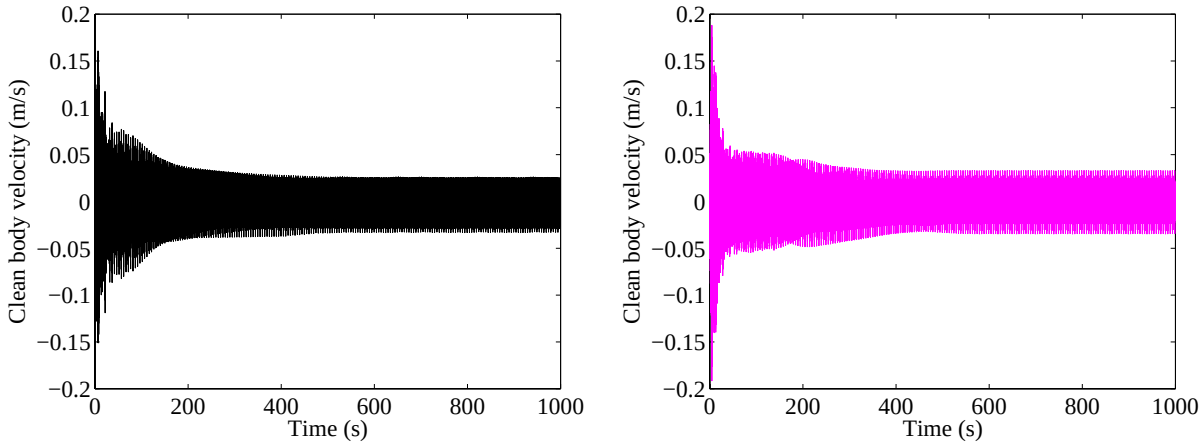


Figure 5: The time history of the clean body velocity during the convergence for two cases

Unless a more sophisticated algorithm is used, the speed of convergence could, in principle, be increased by: a) reducing the time to estimate the time averaged squared velocity, b) increasing the increments, and c) adjusting the ratio of the two increments such that their ratio is equal to the ratio of the optimum, final values for the two control parameters. Figure 6 and Figure 7, which follow that same layout as Figure 4 and Figure 5 show the results for a case when the two increments are increased and adjusted such that the increment in the feedback gain is $inc_g = g_{opt}/10$ and the increment in the blending coefficient is $inc_\alpha = \alpha_{opt}/10$. The time to estimate the mean squared velocity of the clean body is kept the same as in the previous simulation to 5 s.

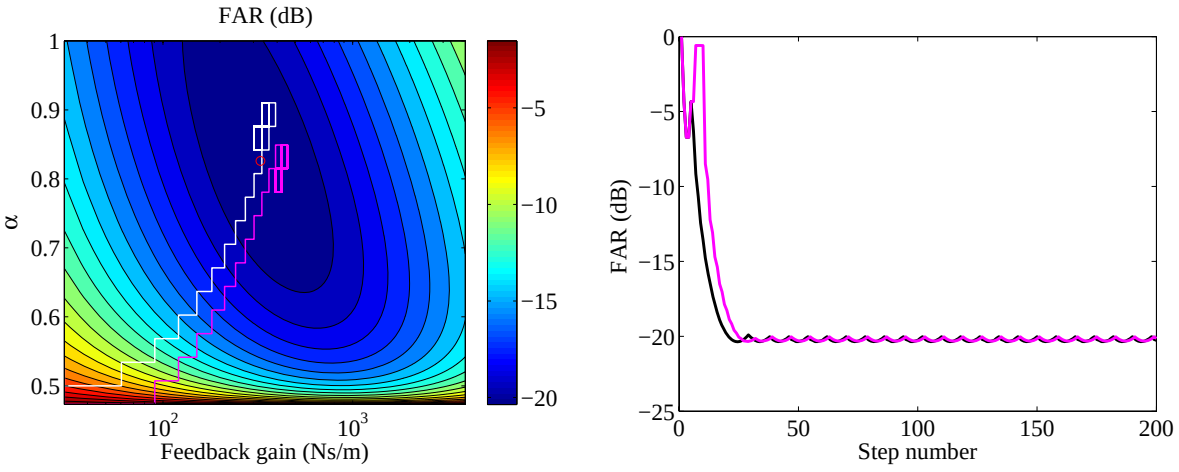


Figure 6: The convergence behaviour of the auto-adaptive controller with increased and adjusted increments

It can be seen in Figure 6 that the convergence trajectory is now more oriented to the minimum of the performance surface, which is due to the adjusted increments for the two control parameters. Also, as shown in the right hand side plot in Figure 6, the convergence occurs after 25 steps. During the remaining 125 steps the algorithm keeps changing the control parameters back and forth around the optimum. Figure 7 shows that the convergence time is now reduced to less than 3 minutes for both cases simulated.

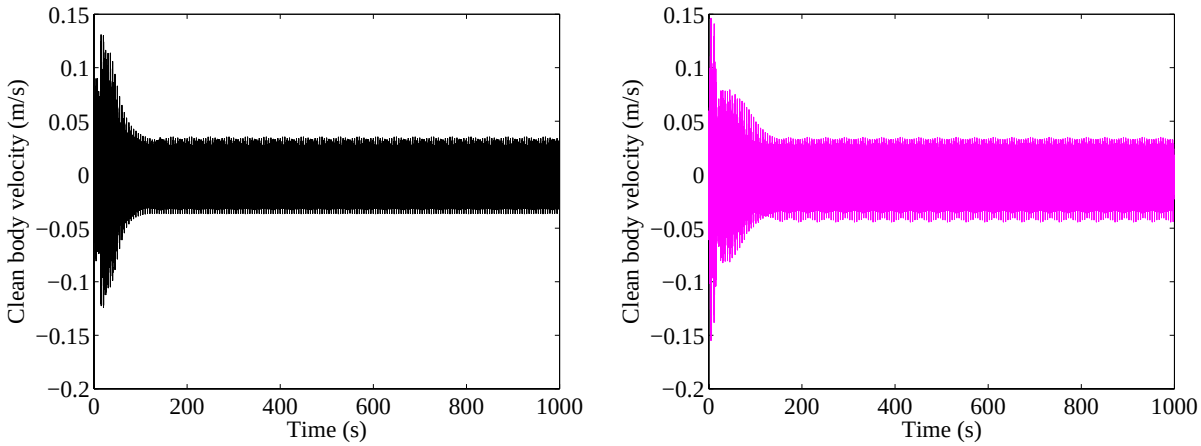


Figure 7: The time history of the clean body velocity during the convergence for two cases with increased and adjusted increments

In Figure 8 and Figure 9 another two results are shown for an algorithm having the same increments as in the previous example. However the time to estimate the mean squared velocity of the clean body is now reduced to 2 s. It can be seen that the speed of convergence is now further improved, as it takes about 30 steps or 60 seconds for the controller to reach the optimum set of control parameters. It can be noted in Figure 8 that with the reduced averaging time there are more backward going steps during the beginning of the convergence process. This is probably because the system at this stage is still quite lightly damped and the reduced averaging time leads to more relative influence of the decaying free vibrations onto the estimated mean squared velocity of the clean body.

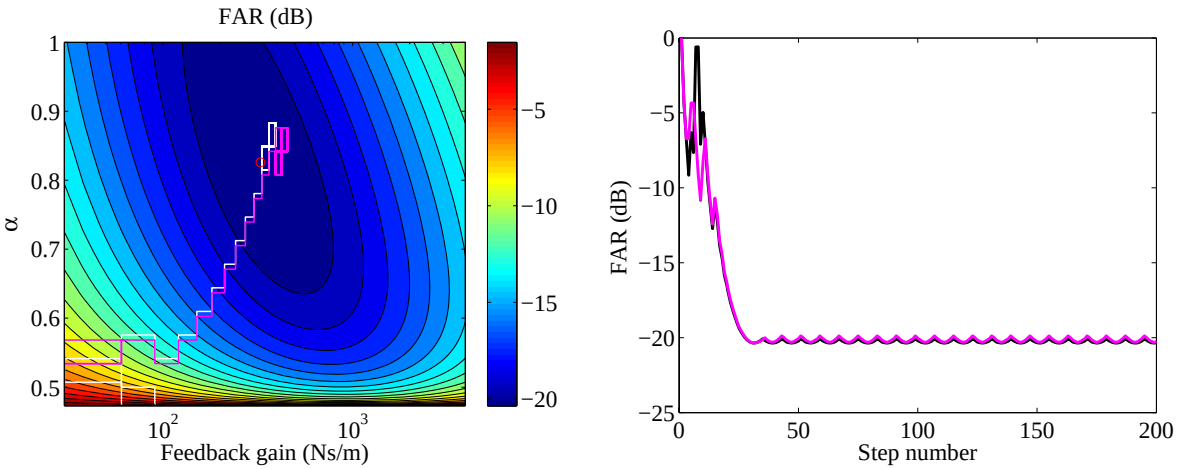


Figure 8: The convergence behaviour of the auto-adaptive controller with increased and adjusted increments, and with decreased averaging time per step.

However, as the damping in the system starts to increase, due to the active damping injected, the mean squared velocity becomes more accurately approximated since the free vibrations decay more quickly.

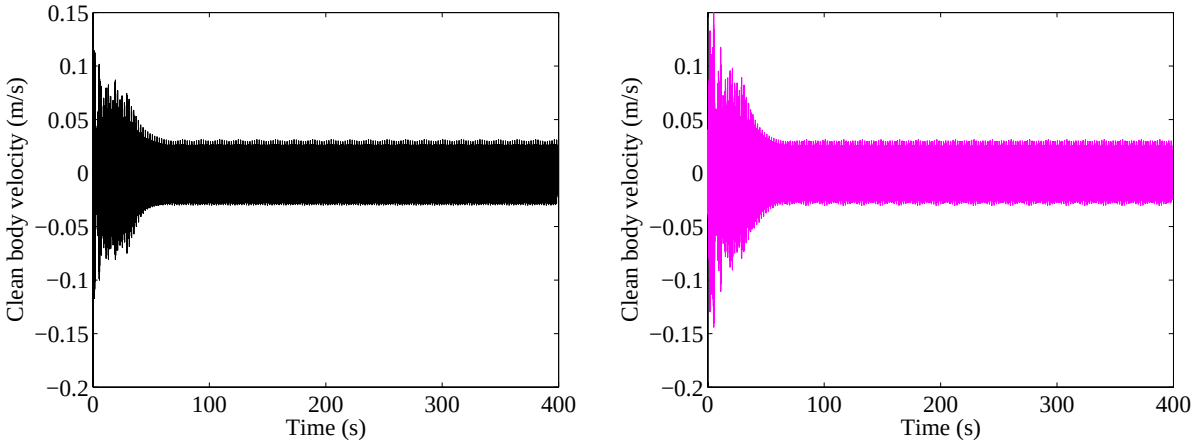


Figure 9: The time history of the clean body velocity during the convergence for two cases with increased and adjusted increments, and with decreased averaging time per step.

In conclusion, the simulation study performed in the time domain with the auto-adaptive blended velocity feedback controller indicates that such an approach is in principle possible. Important parameters for the speed of convergence of the trial and error algorithm are the two control parameter increments, and the time period over which the time averaging of the squared velocity of the clean body is performed. It is important to stress that these algorithm parameters were for the present study determined with some knowledge of the passive system. In fact the optimum pair of feedback gain and the blending coefficient were known a priori. It is not clear how the two increments would be determined for a completely unknown system. Therefore, such an auto adaptive feedback controller might be useful in practical cases where some knowledge exists about the system but which is blurred with some uncertainty. Then it would be good to reach the optimum controller parameters in a number of steps through the described tuning process.

# 5 Conclusions

The study presented is focused onto how to set the correct blending coefficient and the correct feedback gain for active isolation of random vibrations in a subcritical 2dof system, within an automated online process. This is done using a trial and error algorithm which monitors the clean body mean squared vibration velocity and changes the two blended velocity feedback control parameters in order to minimize the clean body vibration in a number of discrete steps.

It is shown in the frequency domain that there is only one combination of the blending coefficient and the feedback gain which yields the optimal vibration isolation. In other words, the isolation performance surface has a global minimum. In addition there are no local minima. It is shown that although in the frequency domain finding the minimum of the performance surface is straightforward, in the time domain the determining of the clean body time-averaged mean squared velocity takes a considerable time per step of the process, such that the convergence of the trial and error algorithm is relatively slow. The series of simulations performed in the time domain with the auto-adaptive blended velocity feedback controller indicate that important parameters to speed up convergence of the trial and error algorithm are the two control parameter increments, and the time period over which the time averaging of the squared velocity of the clean body is performed. Therefore the increments for the feedback gain and the blending coefficient have to be carefully chosen, perhaps using a model-based approach where the optimum feedback gain and the blending coefficient are known a priori but due to a possible uncertainty in the system it is useful to approach the optimum via a number of discrete steps.

## Acknowledgements

The research performed by Neven Alujević was financially supported by the European Commission Marie Curie Reintegration Grant “SPRiNT” and the National MZOS Grant no. 023-0231744-1745. The research performed by Hinko Wolf was financially supported by the National MZOS Grant no. 120-0362321-2198.

## References

[1] A. Preumont, *Vibration Control of Active Structures*, Kluwer Academic, London, (2002).

[2] D. Karnopp, *Active and semi-active vibration isolation*, American Society of Mechanical Engineers, Journal of Mechanical Design 177 (1995) 177–185.

[3] S. J. Elliott, L. Benassi, M. J. Brennan, P. Gardonio, and X. Huang, *Mobility analysis of active isolation systems*, Journal of Sound and Vibration, vol. 271, (2004), pp. 297–321

[4] C. E. Crede, and J. E. Ruzicka, 1996, *Theory of Vibration Isolation*, Chapter 30, C. M. Harris, ed., Shock and Vibration Handbook, McGraw Hill, New York.

[5] E. E. Ungar, 1992, *Vibration Isolation*, Chapter 11, Noise and Vibration Control Engineering, L. Beranek and I. L. Ver, eds., Wiley, Chichester.

[6] S. J. Elliott, M. Serrand, P. Gardonio, *Feedback Stability Limits for Active Isolation Systems with Reactive and Inertial Actuators*, Journal of Vibration and Acoustics, vol. 123 (2001), pp. 250-261.

[7] A. Preumont, A. Francois, F. Bossens and A. Abu-Hanieh, *Force feedback versus acceleration feedback in active vibration isolation*, Journal of Sound and Vibration vol. 257(4), (2002), pp. 605–613

[8] X. Huang, S. J. Elliott, M. J. Brennan, *Active isolation of a flexible structure from base vibration*, Journal of Sound and Vibration vol. 263, (2003), pp. 357–376.

[9] N. Alujevic, H. Wolf, P. Gardonio, and I. Tomac, *Stability and performance limits for active vibration isolation using blended velocity feedback*, Journal of Sound and Vibration vol. 330, (2011), pp. 4981–4997

[10] D. E. Newland: *An introduction to Random Vibrations, Spectral & Wavelet Analysis*, Third Edition, Dover Publications Inc, (2009)